Teach Industrial Robots Peg-Hole-Insertion by Human Demonstration*

Te Tang[1], Hsien-Chung Lin[1], Yu Zhao[1], Yongxiang Fan[1], Wenjie Chen[2] and Masayoshi Tomizuka[1]

Abstract— **Programming robotic assembly tasks usually requires delicate force tuning. In contrast, human may accomplish assembly tasks with much less time and fewer trials. It will be a great benefit if robots can learn the human inherent skill of force control and apply it autonomously. Recent works on Learning from Demonstration (LfD) have shown the possibility to teach robots by human demonstration. The basic idea is to collect the force and corrective velocity that human applies during assembly, and then use them to regress a proper gain for the robot admittance controller. However, many of the LfD methods are tested on collaborative robots with compliant joints and relatively large assembly clearance. For industrial robots, the non-backdrivable mechanism and strict tolerance requirement make the assembly tasks more challenging. This paper modifies the original LfD to be suitable for industrial robots. A new demonstration tool is designed to acquire the human demonstration data. The force control gains are learned by Gaussian Mixture Regression (GMR) and the closed-loop stability is analysed. A series of peg-hole-insertion experiments with H7h7 tolerance on a FANUC manipulator validate the performance of the proposed learning method.**

I. INTRODUCTION

Autonomous assembly is a typical task in industrial production but not easy for robots to execute. Because of the high rigidity and small clearance of the mating parts, even a slight error during assembly will produce a large contact wrench, consequently, failure of operation [1].

In the past years, many active force control methods have been developed for robot assembly. The general idea is to build a compliant controller, which modifies the nominal trajectory on-line to minimize the contact wrench during manipulation [2]–[5]. By convention, force control is to regulate both contact force and torque, where force refers to the three dimensional vector $\boldsymbol{F} = [F_x, F_y, F_z]^T$, and torque refers to the three dimensional vector $\boldsymbol{T} = [T_x, T_y, T_z]^T$. In the following paper, the wrench is utilized to denote both force and torque for description simplicity.

Fig. 1 shows the block diagram of admittance control, which is a common structure for robot force servo [6]. The wrench error $\boldsymbol{w}_e$ generates a set-point for an inner velocity-control loop. The system approaches to steady state when the wrench is regulated to the desired value. Note that when the robot contacts the environment, the closed-loop system dynamics will change accordingly since the environment dynamics are involved. In practice, engineers have to tune the admittance gains on a case by case basis, in order
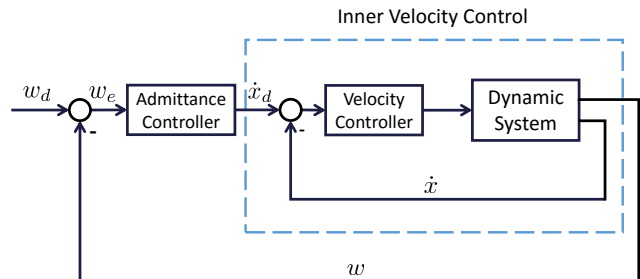
Fig. 1. Force servo with inner velocity control loop

to adapt to the different stiffness, damping or clearance of the environment and to achieve a good force control performance.

In contrast to the non-trivial admittance tuning, human beings could accomplish the assembly task manually with much less time and fewer trials. If regarding this inherent assembly skill inside the human as a controller, then its gains should already be well tuned through our daily operation and experience. Thus the idea to teach robot assembly from human demonstration [7]–[10]. Instead of traditional tuning method, the admittance gains are learned directly from the human, and then applied on the robot force controller.

There are already some preliminary works on learning assembly from human demonstration. In [7], the human assembly skill was modelled as a state-varying admittance and then utilized Gaussian Mixture Regression to predict the corrective velocity from wrench measurement. In [8], a neural network control policy was trained by trial and error and the robot learned to assemble a toy plane with unknown environment dynamics. In [9], the instructor demonstrated the manipulation task in a haptic rendered virtual environment using a haptic device and then used Locally Weighted Projection Regression to model the human corrective trajectory under jamming states.

These methods have shown effective on collaborative robots such as Baxter [11] and PR2 [12], with the assembly tolerance H5h10 or larger. However, few of them are tested on industrial robots. Unlike collaborative robots, the traditional industrial robot is highly rigid because of large gear reduction ratio on the drivetrain. Basically there is no compliance on the mechanism to assist assembly. Besides, the clearance requirement for industrial assembly is more strict. To deal with these problems, we modified our work at [7] to apply learning from demonstration on industrial robots. This paper is organized as follows: Section I introduces the background of autonomous assembly by

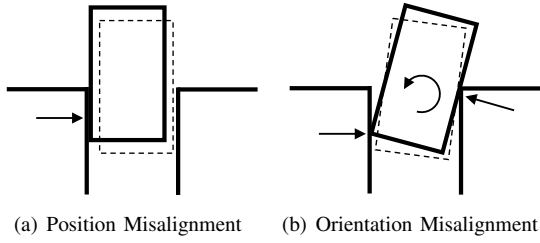(a) Position Misalignment   (b) Orientation Misalignment

Fig. 2. Cross section of peg-hole-insertion. The force/torque feedback signal generates a corresponding translational/rotational velocity command to the robot.

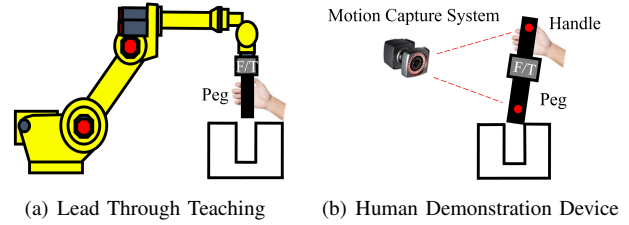(a) Lead Through Teaching   (b) Human Demonstration Device

Fig. 3. Two different methods to acquire human demonstration data.(a) By lead through teaching. Contact wrench is detected by the end-effector F/T sensor, and velocity is calculated by robot forward kinematics; (b) By human demonstration device. Contact wrench is measured by the F/T sensor embedded in HDD, and velocity is measured by the motion capture system.

force control, and the motivation of learning from human demonstration. Section II takes the peg-hole-insertion as an example to analyse the assembly task. A demonstration tool is designed to acquire human demonstration data and the data processing procedures are introduced. Section III introduces a framework of learning the state-varying admittance from human by Gaussian Mixture Regression (GMR). The physical interpretation of GMR is discussed and the closed-loop stability is analysed. A series of experiments are performed on a H7h7 peg-hole testbed and the experimental results are provided in Section IV. Section V is conclusion and discussion.

II. DATA ACQUISITION AND PROCESSING

Peg-hole-insertion, i.e., inserting a round peg into a round hole, is one of the most common assembly tasks in industry. Peg-hole-insertion will be utilized as an example in this paper to introduce how to teach robot assembly skill by human demonstration.

Fig. 2 shows the robot assembly procedure in the cross section. The F/T sensor on the robot end-effector detects the force and torque applied on the peg. By designing a proper control law, the force/torque feedback will generate a corresponding translational/rotational velocity command on the robot end-effector, so as to push the peg away from collision. Similarly, human brain perceives the hand's tactile feedback and then decides which direction to move in order to compliantly assemble the work pieces. However, the human assembly skill is much more sophisticated. Human would apply different admittance according to the different material and tolerance of the work piece, or even according to the different phases during insertion. The core idea of this research is to learn the state-varying admittance by human demonstration data during assembly, and then apply this admittance block to robot force controller.

A. Data Acquisition

The first step of learning from human is to acquire the human demonstration data. For example, how to measure the contact wrench that human feels during assembly? And how to detect the corrective velocity that human applied on the peg? An intuitive idea is to utilize the lead through teaching mode (Fig. 3(a)): human operator grasps the robot end-effector and guides the manipulator to insert the peg into

the hole. During the assembly, the contact force is recorded by the F/T sensor on the end-effector, and the Cartesian space corrective velocity is calculated by the robot forward kinematics. In practice, however, we find that industrial robot's lead though teaching fails in this kind of contact tasks. Since there is usually only one F/T sensor on the industrial robot, it cannot distinguish the wrench applied by the human from that applied by the hole. Therefore the human operator loses control of the robot when the peg starts to contact the hole, and the following insertion procedure cannot be demonstrated.

To deal with this problem, the idea of human demonstration device (HDD [13]) is proposed as shown in Fig. 3(b). Instead of using robot sensors to collect data, an independent tool is designed to collect the required wrench and velocity information. The HDD consists of three major components: from the bottom to the top, a round peg, a F/T sensor and a handle bar. There are also several vision markers attached on for velocity tracking. During human demonstration, human operator grasps the handle bar and performs peg-hole-insertion several trials. The contact wrench and corrective velocity are recorded by the F/T sensor and the motion capture system simultaneously. Section IV will introduce the design of HDD in details.

Compared to lead through teaching, the human operator grasps HDD instead of the robot arm to perform the assembly tasks, which is more natural and intuitive. Second, the robot and human are separated during data acquisition, which ensures the safety of the human operator.

B. Data Processing

As shown in Fig. 4, a Cartesian coordinate is built up with the origin O_S at the center of the F/T sensor. O_P is the Tool Center Point (TCP) at the end of peg. The peg's velocity is described by $\dot{x} = [v_x, v_y, v_z, \omega_x, \omega_y, \omega_z]^T \in \mathbb{R}^6$. The wrench data collected by F/T sensor is $w^S = [F_x^S, F_y^S, F_z^S, M_x^S, M_y^S, M_z^S]^T \in \mathbb{R}^6$.

The collected data set $\dot{x}$ and w^S cannot be directly utilized to train the state-varying admittance. Several data processing steps are required. During peg-hole-insertion, the contact wrench applies at the peg end O_P, but is measured at F/T sensor origin O_S. The measurement value is influenced by the peg length between O_S and O_P. A general assembly skill
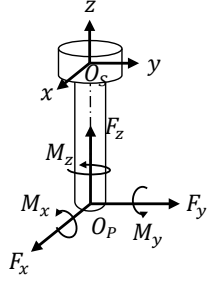
Fig. 4. Wrench applied on the Tool Center Point O_P, while the measurement value is relative to F/T sensor origin O_S.
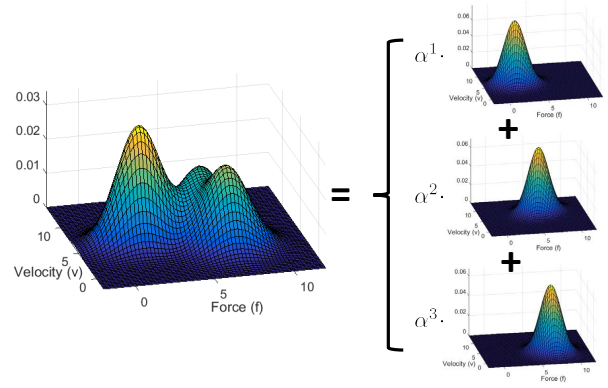

Fig. 5. Estimate data distribution by Gaussian. For the ease of visualization, both velocity and wrench are one dimensional here. The distribution density of the velocity and wrench data collected from human demonstration is shown in the left. This density map is then fitted by superposition of several weighted Gaussian with different means and covariance.

should not be influenced by this specific length. Therefore w^S should be transformed with respect to O_P so as to eliminate the influence of peg length. Denote the wrench at O_P as $w^{TCP} = [F_x, F_y, F_z, M_x, M_y, M_z]^T \in \mathbb{R}^6$. It can be calculated by linear transformation

$$w^{TCP} = \begin{bmatrix} 1 & 0 & 0 & 0 & 0 & 0 \\ 0 & 1 & 0 & 0 & 0 & 0 \\ 0 & 0 & 1 & 0 & 0 & 0 \\ 0 & -\overline{O_S O_P} & 0 & 1 & 0 & 0 \\ +\overline{O_S O_P} & 0 & 0 & 0 & 1 & 0 \\ 0 & 0 & 0 & 0 & 0 & 1 \end{bmatrix} \cdot w^S \quad (1)$$

Besides the convention transformation, if the human operator demonstrates insertions multiple times but with varying speeds, this velocity inconsistency might influence the quality of admittance training. To deal with this problem, the Dynamic Time Warping [14] from speech recognition area can be utilized to synchronize multiple data sets. More details of velocity synchronization can be found in [7].

III. LEARN STATE-VARYING ADMITTANCE BY GAUSSIAN MIXTURE REGRESSION

For a force controller, the admittance gain determines how large the corrective velocity should be according to the measured contact wrench. From Section II, the wrench and velocity information are recorded simultaneously from human demonstration. In this section, we will train an admittance block such that given the same wrench input, it generates a similar velocity output as human does. This is a typical regression problem in statistics. There are many predictors developed for regression, and a question is which would be the most suitable method for our problem?

We set up three criteria to select the proper predictor:

(1) Stability. Since this state-varying admittance block is embedded in the feedback control loop, it could influence the stability of the whole system. The stability conditions of the predictor should be explicitly formulated, so that the system stability can be analysed.

(2) Efficiency. The computation power of industrial robot controller is limited due to cost concerns. It is preferred that the predictor has a closed-form expression so that it could be calculated efficiently on-line.

(3) Interpretation. There are many prediction methods behaving like black boxes. They could generate proper output by learning from training data, but do not have good explanations on their internal dynamics. It is preferred that the predictor in this work has a physical interpretation which explains why it can serve as a state-varying admittance.

Many common predictors, such as neural networks, logistic regression, K-nearest neighbours cannot meet all the above criteria. To meet the three criteria, the Gaussian Mixture Regression (GMR [15]) is introduced in this work to build the state-varying admittance block. In the rest of this section, we will show that GMR has explicit stability conditions, good efficiency and reasonable physical interpretations respectively.

A. Introduction to GMR

The basic idea of GMR is to fit the human demonstration data (sensed wrench w and corrective velocity $\dot{x}_c$) into a joint probability distribution $p(w, \dot{x}_c)$, then use its conditional probability $p(\dot{x}_c|w)$ to retrieve the output $\dot{x}_c$ given the input w.

As shown in Fig. 5, the first step of GMR is to fit the joint probability distribution $p(w, \dot{x}_c)$ by mixture of N Gaussian components, each with mean μ_i, covariance Σ_i and weight α_i, with $\sum_{i=1}^{N} \alpha^i = 1$:

$$p(w, \dot{x}_c) = \sum_{i=1}^{N} \alpha^i p^i(w, \dot{x}_c)$$

$$= \sum_{i=1}^{N} \alpha^i \mathcal{N}\left(\begin{bmatrix} w \\ \dot{x}_c \end{bmatrix} \Big| \begin{bmatrix} \mu_w^i \\ \mu_{\dot{x}_c}^i \end{bmatrix}, \begin{bmatrix} \Sigma_w^i & \Sigma_{w\dot{x}_c}^i \\ \Sigma_{\dot{x}_c w}^i & \Sigma_{\dot{x}_c}^i \end{bmatrix} \right) \quad (2)$$

Since each component $p^i(w, \dot{x}_c)$ is Gaussian, its conditional probability distribution $p^i(\dot{x}_c|w)$ is still Gaussian:

$$p^i(\dot{x}_c|w) = \mathcal{N}(\dot{x}_c|\mu_{\dot{x}_c|w}^i, \Sigma_{\dot{x}_c|w}^i) \quad (3)$$

The overall conditional probability $p(\dot{x}_c|w)$ can be constructed as the sum of each $p^i(\dot{x}_c|w)$, with a weight which

indicates the probability of w belonging to each Gaussian component

$$p(\dot{x}_c|w) = \sum_{i=1}^{N} \frac{\alpha^i \mathscr{N}(w|\mu_w^i, \Sigma_w^i)}{\sum_{j=1}^{N} \alpha^j \mathscr{N}(w|\mu_w^j, \Sigma_w^j)} p^i(\dot{x}_c|w) \qquad (4)$$

To transfer the stochastic probability into a deterministic controller, the admittance block is designed such that given an input wrench w, it will generate an output corrective velocity $\dot{x}_c^*$ that maximizes $p(\dot{x}_c|w)$. $\dot{x}_c^*$ could be calculated from (5) deterministically in real time.

$$\begin{aligned}
\dot{x}_c^* &= \arg\max_{\dot{x}_c} p(\dot{x}_c|w) \\
&= \sum_{i=1}^{N} \frac{\alpha^i \mathscr{N}(w|\mu_w^i, \Sigma_w^i)}{\sum_{j=1}^{N} \alpha^j \mathscr{N}(w|\mu_w^j, \Sigma_w^j)} \mu_{\dot{x}_c|w}^i \\
&= \sum_{i=1}^{N} \frac{\alpha^i \mathscr{N}(w|\mu_w^i, \Sigma_w^i)}{\sum_{j=1}^{N} \alpha^j \mathscr{N}(w|\mu_w^j, \Sigma_w^j)} \left[\mu_{\dot{x}_c}^i + \Sigma_{\dot{x}_c w}^i (\Sigma_w^i)^{-1}(w - \mu_w^i) \right]
\end{aligned}$$
$$(5)$$

The Gaussian parameters $(\mu^i, \Sigma^i, \alpha^i)$ in GMR can be estimated iteratively by E-M algorithm from the human demonstration data $(w, \dot{x}_c)$. More details of GMR parameter calculation can be found in [16].

B. Interpreting GMR with mechanics point of view

The statistic form of GMR as (5) does not provide insight to the dynamic feature of the admittance system [17]. In this section, we rewrite (5) to formulate it like a dynamic system. To simplify the notation, we define:

$$h^i(w) = \frac{\alpha^i \mathscr{N}(w|\mu_w^i, \Sigma_w^i)}{\sum_{j=1}^{N} \alpha^j \mathscr{N}(w|\mu_w^j, \Sigma_w^j)} \qquad (6)$$

$$A^i = \Sigma_{\dot{x}_c w}^i (\Sigma_w^i)^{-1} \qquad (7)$$

where $h^i(w) \in [0,1]$ is a scalar function of w and A^i is a constant square matrix. Substituting (6) and (7) into (5), we have

$$\dot{x}_c = \sum_{i=1}^{N} h^i(w) \left[\mu_{\dot{x}_c}^i + A^i(w - \mu_w^i) \right] \qquad (8)$$

Equation (8) has the following physical interpretation: the state-varying admittance block consists of N linear dampers, where each damper has a unique admittance A^i and a preload velocity $\mu_{\dot{x}_c}^i - A^i \mu_w^i$. Equation (7) reveals the relation between the admittance A^i and the covariance of Gaussian distribution. The nonlinear weight $h^i(w)$ denotes the contribution of each damper to the whole block. If combining multiple dampers into a single nonlinear one, then we can define

$$\bar{A} = \sum_{i=1}^{N} h^i(w) A^i \qquad (9)$$

$$\bar{\mu}_{\dot{x}} = \sum_{i=1}^{N} h^i(w)(\mu_{\dot{x}_c}^i - A^i \mu_w^i) \qquad (10)$$

and $\dot{x}_c$ can be described as

$$\dot{x}_c = \bar{A}w + \bar{\mu}_{\dot{x}} \qquad (11)$$
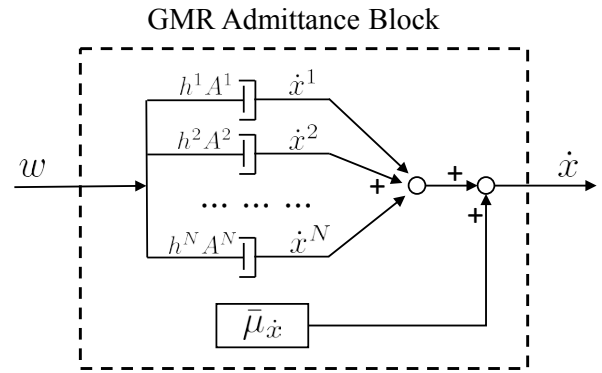

GMR Admittance Block

Fig. 6. Interpretation of GMR in mechanics point of view. The admittance block formulated by GMR consist of N linear dampers with admittance A^i respectively. Each damper has a nonlinear weight $h^i(w)$ denoting its contribution to the whole block. The output of the admittance block is generatd by the summation of the N dampers' outputs as well as an general preload velocity $\bar{\mu}_{\dot{x}}$.

where $\bar{A}$ is the general admittance of the block, and $\bar{\mu}_{\dot{x}}$ is the general preload corrective velocity.

To conclude, the structure of GMR has an inherent similarity with physical admittance systems. It can be interpreted as a combination of multiple dampers with different admittances and nonlinear weights (see Fig. 6). This explicit structure also provides the convenience to analyse the closed-loop stability of the control system.

C. Stability condition of the closed-loop system

For industrial applications, it is a critical issue to guarantee the system stability. This subsection will analyse the stability conditions of the closed loop system with GMR based on Lyapunov theorem [18].

Theorem 1. Consider a closed loop robot control system (Fig. 7) consisting of a robot, an admittance control block $\dot{x}_c = \sum_{i=1}^{N} h^i(w_e) \left[\mu_{\dot{x}_c}^i + A^i(w_e - \mu_w^i) \right]$, a velocity controller $\tau_v = K_P(\dot{x}_c - \dot{x}) - K_I x$, a gravity compensator, and damped environment $w = K_d \dot{x}$. The closed-loop system is asymptotically stable at $(x, \dot{x}) = 0$ if:

$$K_P \succeq 0 \qquad (12)$$

$$K_I \succ 0 \qquad (13)$$

$$\bar{\mu}_{\dot{x}} = 0 \qquad (14)$$

$$K_P A^i K_d \succeq 0 \qquad \forall i = 1, 2, \cdots, N \qquad (15)$$

Proof :

First define a Lyapunov function

$$V = \frac{1}{2} x^T K_I x + \frac{1}{2} \dot{x}^T M_x(x) \dot{x} \qquad (16)$$

where x and $\dot{x}$ are the position and velocity of the robot end-effector. $M_x(x)$ is the robot inertia matrix in Cartesian space. Since $K_I \succ 0$ and $M_x(x) \succ 0$, therefore $V > 0$. Take derivative of (16) and obtain

$$\dot{V} = \dot{x}^T K_I x + \frac{1}{2} \dot{x}^T \dot{M}_x(x, \dot{x}) \dot{x} + \dot{x}^T M_x(x) \ddot{x} \qquad (17)$$
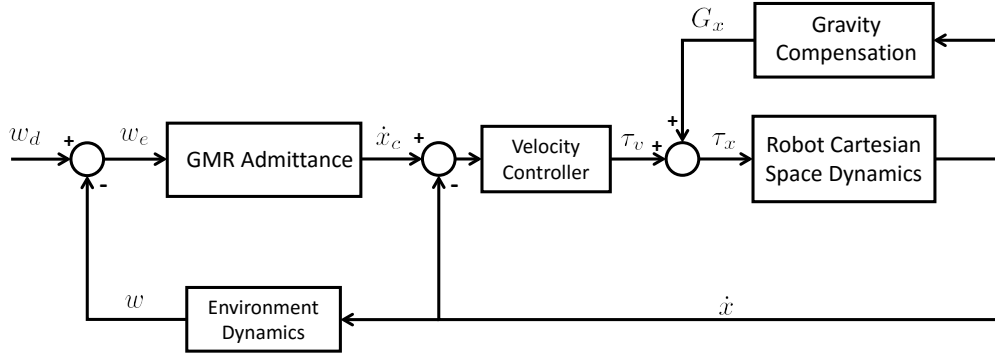
Fig. 7. Force Control Block Diagram with GMR Admittance Module.

In Cartesian space, take the robot dynamic equation

$$M_x(x)\ddot{x} + C_x(x,\dot{x})\dot{x} + G_x(x) = \tau_x \quad (18)$$

where $C_x(x,\dot{x})$ is the Coriolis matrix, $G_x(x)$ is the gravity term, and τ_x is the control input. $\dot{M}_x(x,\dot{x}) - 2C_x(x,\dot{x})$ keeps the property of skew-symmetry as in the joint space, thus

$$\dot{x}^T \left[\dot{M}_x(x,\dot{x}) - 2C_x(x,\dot{x}) \right] \dot{x} = 0 \quad \forall \dot{x} \quad (19)$$

Substitute (18) and (19) into (17) to get

$$\dot{V} = \dot{x}^T K_I x + \frac{1}{2}\dot{x}^T \left[\dot{M}_x(x,\dot{x}) - 2C_x(x,\dot{x}) \right] \dot{x} + \dot{x}^T [\tau_x - G_x(x)]$$
$$= \dot{x}^T [\tau_x - G_x(x) + K_I x] \quad (20)$$

For the Cartesian space control law,

$$\tau_x = \tau_v + G_x(x)$$
$$= K_P[\dot{x}_c - \dot{x}] - K_I x + G_x(x)$$
$$= K_P\{\sum_{i=1}^{N} h^i(w_e) \left[\mu_{\dot{x}_c}^i + A^i(w_e - \mu_w^i) \right] - \dot{x}\} - K_I x + G_x(x)$$
$$= K_P \left[\sum_{i=1}^{N} h^i(w_e)A^i w_e + \bar{\mu}_{\dot{x}} - \dot{x} \right] - K_I x + G_x(x) \quad (21)$$

The desired contact wrench w_d is zero, therefore $w_e = w_d - K_d\dot{x} = -K_d\dot{x}$. Also from the stability condition, $\bar{\mu}_{\dot{x}} = 0$. Substitute the relation into (21) to obtain

$$\tau_x = -K_P \left[\sum_{i=1}^{N} h^i(w_e)A^i K_d + I \right] \dot{x} - K_I x + G_x(x) \quad (22)$$

Substituting (22) into (20), we obtain

$$\dot{V} = -\dot{x}^T \left[\sum_{i=1}^{N} h^i(w_e)K_P A^i K_d + K_P \right] \dot{x} \quad (23)$$

Since $K_P \succeq 0$, $K_P A^i K_d \succeq 0$ and $h^i(w_e) \in [0,1]$, the superposition $[\sum_{i=1}^{N} h^i(w_e)K_P A^i K_d + K_P]$ should also be positive semi-definite. Therefore $\dot{V} \leq 0$, and the closed-loop system is Lyapunov stable at $(x,\dot{x}) = 0$. By further applying LaSalle's Invariance Principle on this autonomous system, it is found that the largest invariant set contains the only equilibrium point $(x,\dot{x}) = 0$. Finally, we can conclude that the closed-loop system is asymptotically stable at $(x,\dot{x}) = 0$.
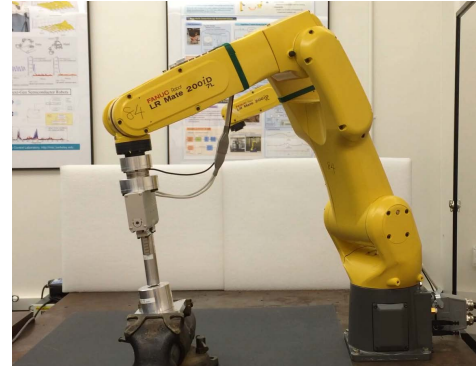

Fig. 8. Peg-Hole-Insertion Testbed.

Note that the above is a sufficient condition for closed-loop stability, and the assumptions in the theorem is conservative. It requires the environment to contain only damping terms. But in many cases, the environment also contains stiffness terms. Besides, the positive semi-definite condition in (15) is not easy to achieve. However, if we have the value of K_d, then we can choose $K_P = K_d^T$ to satisfy (15), which can be proved by Cholesky decomposition.

IV. EXPERIMENTS AND RESULTS

To demonstrate the performance of the proposed learning method, a series of experiments are performed on industrial robot FANUC LR Mate 200iD/7L. The experimental video can be found in [19].

The testbed is shown in Fig. 8. The peg and hole are both machined from Aluminium 6061-T6, with a peg diameter of 0.999in (25.370mm), a hole diameter of 1.000in (25.400mm) and 1.0mm chamfers. The assembly tolerance is industrial standard H7h7.

To collect the human demonstration data, the HDD device (see Fig. 9) is designed. The ATI-Mini45 F/T sensor [20] is embedded between peg and handle bar to collect the wrench information that human perceives during demonstration. The PhaseSpace motion capture system [21] with five active makers on HDD records the corrective velocity that human applies on the peg.
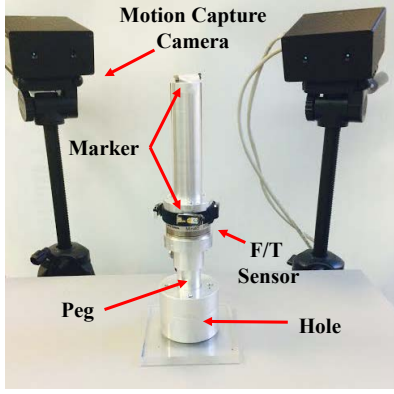
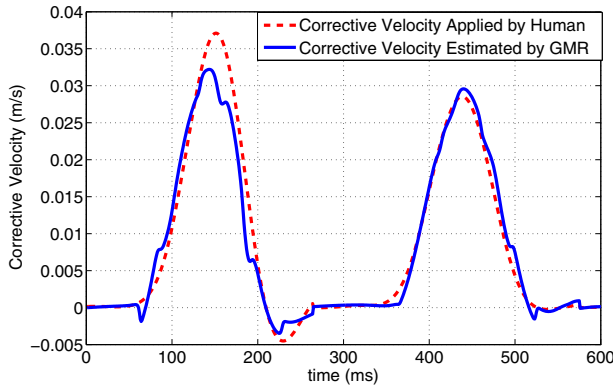Fig. 9.   Human Demonstration Device (HDD) for Data Acquisition.

Fig. 10.   Prediction Performance of GMR on Test Data.

In the human demonstration phase, human demonstrates peg-hole-insertion 50 times from random initial poses. The wrench w and corrective velocity $\dot{x}_c$ are recorded with sampling frequency 1kHz and 960Hz respectively. The two data sets with different frequencies are then synchronized by linear interpolation and smoothed by a moving average filter.

In peg-hole-insertion task, the rotational velocity around peg axis is usually fixed to be zero ($\omega_z = 0$), and translational velocity along peg axis is defined manually as task requirement. Here, $v_z = \max\{0, 0.01(1 - F_z/20)\}$. So insertion is at a 0.01m/s feeding speed along the peg axis if there is no resistance force F_z, and slows down linearly when F_z increases. If $F_z \geq 20N$, the robot will stop feeding. The velocity command for other four dimensional $[v_x, v_y, \omega_x, \omega_y]$ is calculated by the GMR admittance block.

For the admittance block training, fifteen Gaussian components ($N = 15$) are used in the GMR model. The Gaussian parameters are initialized by K-means clustering and iteratively optimized by E-M algorithm. Fig. 10 shows the GMR's performance on test data. For the same wrench input, the red dashed line is the corrective velocity applied by human, and the blue solid line is the GMR output. The average estimation error is 0.213mm/s, with standard variation of 2.2mm/s.

It is the misalignment between the peg and hole that makes

Fig. 11.   Process of Robot Autonomous Insertion with Initial Orientation Misalignment.

TABLE I

EXPERIMENTAL RESULT OF ROBOT AUTONOMOUS INSERTION UNDER FOUR DIFFERENT CONDITIONS.

	Success Rates (%)	Avg. Cycle Time (s)	Avg. Contact Force (N)	Avg. Contact Torque (N.m)
(a)	100.0	2.2	1.87	0.023
(b)	100.0	2.3	2.03	0.025
(c)	96.0	2.8	1.91	0.032
(d)	96.0	2.8	2.21	0.030

the insertion task difficult. Therefore in experiment, we introduce an initial misalignment on purpose to test the proposed learning method. The robot performs autonomous insertions in the following four groups with different misalignment conditions.

(a) Small position misalignment ($\pm 1mm$), and small orientation misalignment ($\pm 1°$).
(b) Large position misalignment ($\pm 2mm$), and small orientation misalignment ($\pm 1°$).
(c) Small position misalignment ($\pm 1mm$), and large orientation misalignment ($\pm 3°$).
(d) Large position misalignment ($\pm 2mm$), and large orientation misalignment ($\pm 3°$).

There are 25 trails in each group and the insertion depth is 20mm in each trial. The process of the robot autonomous insertion is illustrated in Fig. 11. This trial of insertion starts with a large orientation error. The robot succeeds to correct the orientation by the trained state-varying admittance block. Table I shows the experimental results under the four specified conditions. The success rates are all over 96%, which indicates the robot force control could generate proper commands to adjust the peg's pose during insertion. The best performance is achieved (100% success rate) when there is small orientation misalignment. The success rate drops to 96% for large orientation misalignment. This indicates that the proposed learning method is relatively non-sensitive to position misalignment, but more sensitive to orientation misalignment.

Fig. 12 and Fig. 13 show the force and torque plots during one trial of insertion. Contacting happens at 0.25s, and large force and torque occur during contact with peak force 5.71N and peak torque 0.085Nm. The force controller then takes action and regulates both force and torque towards zero. The residual force error is less than 0.41N and residual torque is less than 0.006Nm. Total insertion time is 2.43s.

To conclude, the proposed LfD method is suitable for non-backdrivable industrial robots and performs well on
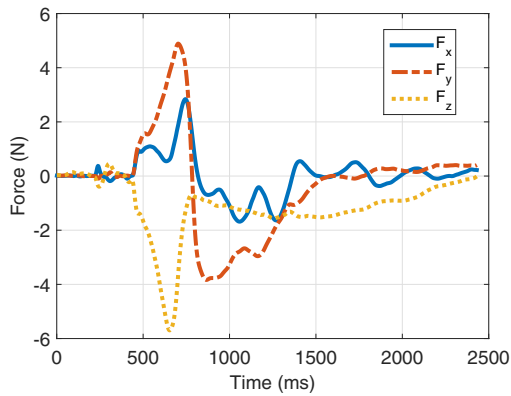
Fig. 12. Force Plot During One Trial of Peg-Hole-Insertion.
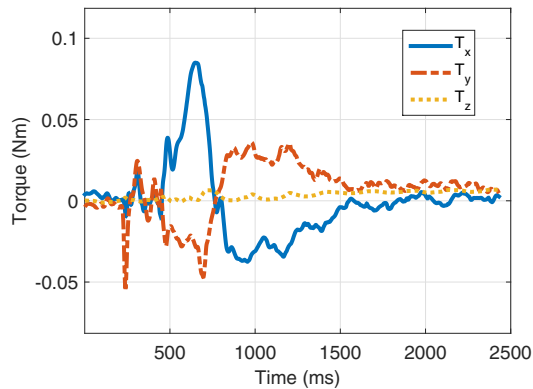

Fig. 13. Torque Plot During One Trial of Peg-Hole-Insertion.

peg-hole-insertion tasks with industrial tolerance standard (H7h7). Traditional force control methods, if well tuned, can also regulate the contact wrench very well and achieve high success rate. However, the major advantage of our method is to eliminate the gain tuning process on the robot. The admittance gains in the force controller are directly learned from human demonstration data. The demonstration process is safe, efficient and intuitive. Moreover, since there is no tuning process, this method does not require high skills or expertise on the robot operator.

V. CONCLUSIONS

In this paper, a framework of teaching industrial robots peg-hole-insertion by human demonstration is introduced. Instead of manually tuning the admittance gain in force controller, this paper introduced Gaussian Mixture Regression (GMR) to learn the state-varying admittance directly from human demonstration data. A human demonstration device (HDD) is designed to collect the wrench and corrective velocity information during demonstration. The efficiency, physical interpretation and stability conditions of the GMR admittance module are analysed. A series of experiments performed on a FANUC industrial robot and a H7h7 tolerance testbed demonstrate the effectiveness of the proposed learning framework. The success rate is better than 96%

with $\pm 2mm$ initial position misalignment and $\pm 3°$ initial orientation misalignment.

REFERENCES

[1] M. A. Peshkin, "Programmed compliance for error corrective assembly," *Robotics and Automation, IEEE Transactions on*, vol. 6, no. 4, pp. 473–482, 1990.
[2] I.-W. Kim, D.-J. Lim, and K.-I. Kim, "Active peg-in-hole of chamferless parts using force/moment sensor," in *Intelligent Robots and Systems, 1999. IROS'99. Proceedings. 1999 IEEE/RSJ International Conference on*, vol. 2. IEEE, 1999, pp. 948–953.
[3] S. R. Chhatpar and M. S. Branicky, "Search strategies for peg-in-hole assemblies with position uncertainty," in *Intelligent Robots and Systems, 2001. Proceedings. 2001 IEEE/RSJ International Conference on*, vol. 3. IEEE, 2001, pp. 1465–1470.
[4] G. Morel, E. Malis, and S. Boudet, "Impedance based combination of visual and force control," in *Robotics and Automation, 1998. Proceedings. 1998 IEEE International Conference on*, vol. 2. IEEE, 1998, pp. 1743–1748.
[5] D. E. Whitney, "Historical perspective and state of the art in robot force control," *The International Journal of Robotics Research*, vol. 6, no. 1, pp. 3–14, 1987.
[6] J. J. Craig, *Introduction to robotics: mechanics and control*. Pearson Prentice Hall Upper Saddle River, 2005, vol. 3.
[7] T. Tang, H.-C. Lin, and M. Tomizuka, "A learning-based framework for robot peg-hole-insertion," in *ASME 2015 Dynamic Systems and Control Conference*. American Society of Mechanical Engineers, 2015, pp. V002T27A002–V002T27A002.
[8] S. Levine, N. Wagener, and P. Abbeel, "Learning contact-rich manipulation skills with guided policy search," in *Robotics and Automation (ICRA), 2015 IEEE International Conference on*. IEEE, 2015, pp. 156–163.
[9] Y. Chen, X. Han, M. Okada, Y. Chen, and F. Naghdy, "Intelligent robotic peg-in-hole insertion learning based on haptic virtual environment," in *Computer-Aided Design and Computer Graphics, 2007 10th IEEE International Conference on*. IEEE, 2007, pp. 355–360.
[10] K. Kronander, E. Burdet, and A. Billard, "Task transfer via collaborative manipulation for insertion assembly," in *Workshop on Human-Robot Interaction for Industrial Manufacturing, Robotics, Science and Systems*. Citeseer, 2014.
[11] Baxter from Rethink Robotics, "http://www.rethinkrobotics.com."
[12] PR2 from Willow Garage, "https://www.willowgarage.com."
[13] H.-C. Lin, T. Tang, *et al.*, "Remote lead through teaching by human demonstration device," in *ASME 2015 Dynamic Systems and Control Conference*. American Society of Mechanical Engineers, oct 2015.
[14] H. Sakoe and S. Chiba, "Dynamic programming algorithm optimization for spoken word recognition," *Acoustics, Speech and Signal Processing, IEEE Transactions on*, vol. 26, no. 1, pp. 43–49, 1978.
[15] C. M. Bishop, "Pattern recognition," *Machine Learning*, 2006.
[16] J. A. Bilmes *et al.*, "A gentle tutorial of the em algorithm and its application to parameter estimation for gaussian mixture and hidden markov models," *International Computer Science Institute*, vol. 4, no. 510, p. 126, 1998.
[17] S. M. Khansari-Zadeh, K. Kronander, and A. Billard, "Modeling robot discrete movements with state-varying stiffness and damping: A framework for integrated motion generation and impedance control," *Proceedings of Robotics: Science and Systems X (RSS 2014)*, 2014.
[18] J.-J. E. Slotine, W. Li, *et al.*, *Applied nonlinear control*. Prentice-Hall Englewood Cliffs, NJ, 1991, vol. 199, no. 1.
[19] Experimental Video, http://me.berkeley.edu/~tetang/AIM2016/PegInHole.html.
[20] ATI Mini45 F/T sensor, "http://www.ati-ia.com/Products/ft."
[21] Impulse Motion Capture System from PhaseSpace Inc., "http://www.phasespace.com/index.html."